Rate of Phosphate Release after Photoliberation of Adenosine 5′-Triphosphate in Slow and Fast Skeletal Muscle Fibers

Z.-H. He,* G. J. M. Stienen,# J. P. F. Barends,# and M. A. Ferenczi*
*National Institute for Medical Research, The Ridgeway, Mill Hill, London NW7 1AA, United Kingdom, and #Laboratory for Physiology, Institute for Cardiovascular Research, Free University, 1081 BT Amsterdam, the Netherlands

ABSTRACT Inorganic phosphate (P_i) release was determined by means of a fluorescent P_i-probe in single permeabilized rabbit soleus and psoas muscle fibers. Measurements of P_i release followed photoliberation of ~1.5 mM ATP by flash photolysis of NPE-caged ATP in the absence and presence of Ca^{2+} at 15°C. In the absence of Ca^{2+}, P_i release occurred with a slow rate of 11 ± 3 $\mu M \cdot s^{-1}$ ($n = 3$) in soleus fibers and 23 ± 1 $\mu M \cdot s^{-1}$ ($n = 10$) in psoas fibers. At saturating Ca^{2+} concentrations (pCa 4.5), photoliberation of ATP was followed by rapid force development. The initial rate of P_i release was 0.57 ± 0.05 $mM \cdot s^{-1}$ in soleus ($n = 13$) and 4.7 ± 0.2 $mM \cdot s^{-1}$ in psoas ($n = 23$), corresponding to a rate of P_i release per myosin head of 3.8 s^{-1} in soleus and 31.5 s^{-1} in psoas. P_i release declined at a rate of 0.48 s^{-1} in soleus and of 5.2 s^{-1} in psoas. P_i release in soleus was slightly faster in the presence of an ATP regenerating system but slower when 0.5 mM ADP was added. The reduction in the rate of P_i release results from an initial redistribution of cross-bridges over different states and a subsequent ADP-sensitive slowing of cross-bridge detachment.

INTRODUCTION

Force production in muscle takes place via the molecular interaction between the myosin heads and their binding sites on actin filaments. This continuous process of formation and breakage of bonds, the cross-bridge cycle, is driven by the free energy change associated with ATP breakdown to ADP and inorganic phosphate (P_i). Previous determinations of the energetic cost of force production in intact muscle were mainly based on oxygen consumption or heat production associated with ATP utilization and re-synthesis (Woledge et al., 1985). More direct measurements of the rate of ATP hydrolysis were performed in skinned muscle fibers—from which the surface membrane was removed—and in isolated myofibrils, either from the amount of inorganic phosphate or ADP produced, by enzymatic coupling of the ATP re-synthesis with the breakdown of NADH or oxygen isotope exchange (Glyn and Sleep, 1985; Kawai et al., 1987; Lionne et al., 1995; Potma et al., 1994a, b; 1995; Potma and Stienen, 1996; Stienen et al., 1990; Webb et al., 1986). These methods revealed a fairly consistent picture of ATP hydrolysis, and the variation thereof, in different fiber types during isometric contractions.

The time resolution of these measurements, however, is limited to ~1 s. Heat measurements are most favorable in this respect but they are rather indirect, require extensive averaging and correction, and even then are limited to 10–100-ms time resolution. A major step forward was made by the development of a fluorescent P_i-probe (MDCC-PBP), a genetically engineered A197C mutant of the phosphate binding protein (PBP) of *Escherichia coli* labeled with *N*-(2-[1-maleimidyl]ethyl)-7-diethylaminocoumarin-3-carboxamide (MDCC). This probe allows measurement of the rate of P_i splitting with millisecond time resolution (Brune et al., 1994; Corrie, 1994). This method has been validated and applied recently in skinned rabbit psoas muscle fibers (Ferenczi et al., 1995; He et al., 1997). The affinity of the phosphate binding protein for phosphate is high ($K_d = 0.15$ μM) so that P_i binding is essentially irreversible. The maximum amount of P_i that can be detected depends on the amount of phosphate binding protein in the solution or the fiber. In practice, this is no more than 2 mM. To study ATP hydrolysis associated with the actomyosin interaction, the muscle fibers have to be activated quickly, e.g., by means of photolysis of caged compounds, to avoid saturation of the probe.

The results obtained by Ferenczi et al. (1995) and He et al. (1997) were striking in that they revealed that after photolysis of caged ATP, the initial rate of P_i release was ~10 times faster than the steady-state ATP hydrolysis rate observed by others. He et al. (1997) also showed that during the initial phase of contraction, the rate of P_i release declined with time, but saturation of the P_i-probe occurred before a steady state was reached. In these experiments, during the period of highest ATPase activity, the concentration of ATP and of ADP in the fibers was not constant (the ATP concentration decreased and ADP accumulated) despite the presence of high concentrations of an ATP regenerating system (creatine kinase and phosphocreatine). Here we aimed to investigate the rate of P_i release until the steady-state rate is established. The steady-state ATPase rate in slow muscle fibers of the rabbit is well characterized and about a factor of 7 slower than in the fast rabbit psoas fibers; hence, saturation of the probe will occur much more slowly. Also, the ATP regenerating system will be able to maintain a near-constant concentration of ATP and ADP,

Received for publication 24 February 1998 and in final form 30 June 1998.
Address reprint requests to Dr. G. J. M. Stienen, Laboratory for Physiology, Free University, van der Boechorststraat 7, 1081 BT Amsterdam, The Netherlands. Tel.: 31-20-4448122; Fax: 31-20-4448255; E-mail: gjm.stienen.physiol@med.vu.nl.

0006-3495/98/11/2389/13 $2.00

thus allowing us to investigate more rigorously the role of ADP in controlling ATPase activity than was possible in psoas fibers (He et al., 1997). An additional goal of the investigation was to make a direct comparison between the rate of P_i release and the force responses after photolysis of caged ATP in slow and fast fibers under conditions very similar to those used by Potma et al. (1994a, b; 1995). This allowed us to test and to extend the kinetic scheme for cross-bridge interaction used in those studies.

METHODS

Preparations

Fiber bundles were quickly dissected from rabbit soleus and psoas muscles. These bundles were tied to wooden applicator sticks at rest length. The muscle fibers were permeabilized as described by Thirlwell et al. (1994) and stored in a relaxing solution containing 50% glycerol at −18°C for up to 4 weeks. From these bundles, single fiber segments were isolated and mounted in the experimental set-up by means of aluminum T-clips (Goldman and Simmons, 1984). Before mounting, the ends of the fiber segments were cross-linked with a 0.5% glutaraldehyde in rigor solution to improve their stability and mechanical performance (Chase and Kushmerick, 1988). One end of the fiber was attached to a force transducer (AE801, SensoNor, Horten, Norway). The other end was fixed to a micromanipulator to allow adjustment of fiber length.

After mounting, the fibers were kept in relaxing solution to which 1% vol/vol Triton X-100 was added for at least 1 h, to disrupt remaining membrane fragments and remove sarcoplasmic reticulum ATPase activity (cf. Potma et al., 1994a, b). Sarcomere length, measured in relaxing solution by helium-neon laser diffraction, was adjusted to 2.4 μm. The width and depth of the fiber were measured microscopically at a 1000× magnification. Cross-sectional area was calculated assuming an elliptical cross-section.

P_i release and force measurements

The apparatus used to measure P_i release and force was as described previously (Ferenczi et al., 1995; He et al., 1997). Briefly, single fibers were mounted in one of an assembly of six stainless steel troughs (30 μl), built on the temperature-controlled stage of a Zeiss ACM microscope (ACM, Zeiss, Oberkochen, Germany), which was kept at 15°C. The microscope was equipped with an epifluorescence attachment that used a tungsten lamp for excitation of the P_i-probe (MDCC-PBP) at 420 nm. A Zeiss 40× water immersion objective (0.75 NA) was used to illuminate the fiber and to collect fluorescence through a dichroic mirror in an area 150 μm in diameter. Fluorescence from MDCC-PBP at 470 nm was measured by means of a photomultiplier mounted on the microscope head. One of the troughs had a quartz window to allow illumination of the fiber by means of a frequency doubled ruby laser (Lumonics Ltd., Rugby, U.K.) which produced 30-ns light pulses at 347 nm with an energy of ~100 mJ focused onto the fiber by means of a cylindrical lens. During photolysis and subsequent measurements, the fiber segment was bathed in silicone oil to reduce background fluorescence. A single pulse from the laser photolyzed the P^3-1-(2-nitrophenyl)ethyl ester of ATP (NPE-caged ATP) and released ~1.5 mM ATP inside the fiber. Occasionally, repeated flashes were given to ascertain that the amount of ATP released was not limiting the P_i release measurements. The force and fluorescence signals were recorded on a chart recorder, a digital oscilloscope and, after analog-to-digital conversion at 4 kHz, on a personal computer.

Experimental solutions and protocol

MDCC-PBP, the A197C mutant of the *E. coli* phosphate binding protein labeled with *N*-(2-[1-maleimidyl]ethyl)-7-diethylaminocoumarin-3-carboxamide, was prepared as described by Brune et al. (1994) and Corrie (1994). Concentrations given are those of the active protein (He et al., 1997). All solutions were handled with care to minimize P_i contamination. P_i contamination was reduced to micromolar levels by treatment of the solutions and the fiber with 0.5–1 mM 7-methylguanosine (MEG) and 1 U/ml purine nucleoside phosphorylase (PNPase) for at least 10 min (cf. Brune et al., 1994). NPE-caged ATP was synthesized by the method of Walker et al. (1989) and purified by the method of Corrie and Reid (1995).

The fibers were mounted in a relaxing solution consisting of 5 mM MgATP, 60 mM TES (2-*N*-tris[hydroxymethyl]methyl-2-amino)ethanesulfonic acid (pH 7.1, adjusted with KOH), 20 mM EGTA (ethylene glycol bis-[β-aminoethyl ether]-*N,N,N′,N′*-tetraacetic acid), 1 mM free Mg^{2+}, and 20 mM glutathione. Ionic strength was adjusted to 150 mM with potassium propionate. Fibers were then immersed in a Ca^{2+}-free rigor solution (as relaxing solution without ATP, with MEG/PNPase), in which rigor force developed and P_i was removed. The subsequent step in the protocol (the loading solution) depended on the specific aim of the experiment. To study basal P_i release, fibers were transferred to rigor solution with 5 mM NPE-caged ATP and either 0.6 or 1.2 mM MDCC-PBP. To study P_i release during active force development, the 20 mM EGTA was replaced with 20 mM CaEGTA to achieve pCa 4.5 (31.6 μM Ca^{2+}). Finally, the fibers were transferred to the trough with quartz windows containing silicone oil and the laser was fired. After photolysis, the fiber was transferred back to relaxing solution and the cycle was repeated two to four times.

In most cases, the experiments were performed in the absence of an ATP regenerating system. This implies that ATP hydrolysis inside the fiber results in a gradual decrease in ATP concentration and an equivalent accumulation of ADP. Soleus fibers have a higher affinity for ADP than psoas fibers (Horiuti et al., 1997). Therefore, in a separate set of experiments on soleus fibers we investigated the effects of the reduction in ATP concentration and the increase in ADP concentration by using an ATP regenerating system consisting of 10 mM creatine phosphate and 4 mg/ml creatine kinase from chicken skeletal muscle (activity 338 U/mg protein at 25°C, pH 7; Bershitsky et al., 1996). Assuming a twofold reduction of creatine kinase activity at 15°C, this activity would correspond to a maximum rate of ATP regeneration of 11 mM · s^{-1} at 15°C. The NPE-caged ATP stock solution was pretreated with apyrase (20 U · ml^{-1}), as described by Thirlwell et al. (1994), to minimize ATP contamination. The final apyrase concentration in the loading solution amounted to 0.9 U · ml^{-1}. The ADP dependence of P_i release and force development was also studied by adding 0.5 mM Na_2ADP to the loading solutions (without apyrase). For experiments in the presence of ADP, the ADP-containing trials were carried out before the ADP-free trials, as the latter required apyrase, and we found that once added to the fibers, apyrase could not be satisfactorily removed.

Sarcomere length changes

In one experiment the helium-neon laser diffraction pattern was recorded from a central area of the fiber to study the effect of end compliance residing in the connections between the fiber ends and the set-up. A beam of laser light (wavelength 634 nm) was projected onto the fiber and the position of the first-order diffraction line was recorded by means of a position-sensitive photodiode (PS-100-10; Quantrad, Santa Clara, CA) at a distance of 170 mm from the fiber. The position signal was calibrated before the laser was fired by moving the photodiode laterally by a measured distance, and recording the output signal while the fiber, preincubated in the NPE-caged ATP containing activating solution, was kept in oil.

Data analysis

The amplitude of the fluorescence signal depends on the fiber volume in the field of view, on the concentration of MDCC-PBP in the fiber, and on the degree of saturation of the probe with P_i. The fluorescence of MDCC-

PBP saturated with P_i is four to fivefold greater than for the P_i-free probe under the pertaining experimental conditions. Previous work has shown that the amplitude of the fluorescence signal is proportional to the amount of P_i present (Fig. 1 of He et al., 1997), so the concentration of P_i, and hence the rate of P_i released, were derived from the fluorescence signal after subtraction of the fluorescence background recorded during a period before the laser fired. The signal was normalized to the fluorescence signal obtained after MDCC-PBP was saturated (the latter was also corrected for background), and multiplied by the MDCC-PBP concentration. The amount of P_i released by the fiber is related to the amplitude of the fluorescence signal by

$$[P_i] = (F_t - F_{min}) \times [\text{MDCC-PBP}]/(F_{max} - F_{min}) \quad (1)$$

where $[P_i]$ is the concentration of P_i released in the fiber and indicates MDCC-PBP-bound P_i (in mM), F_t is the amplitude of the fluorescence signal at time t, F_{min} is the fluorescence signal before photolytic release of ATP, F_{max} is the fluorescence signal when all the MDCC-PBP is saturated with P_i, and [MDCC-PBP] is the concentration of P_i-probe in the muscle fiber (in mM). The above relationship does not hold when the amount of P_i released is close to, or exceeds, the amount of MDCC-PBP in the fiber.

Upon photolysis of NPE-caged ATP a short-lived *aci*-nitro intermediate is formed which absorbs light at 420 nm (Corrie et al., 1992). This caused an abrupt decrease in the fluorescence signal immediately after the flash, which at 15°C recovers with a rate constant of 57.6 s^{-1}, and a small decrease in the apparent steady-state fluorescence because of increased absorption of the solution (inner-filter effect). The artifact was seen previously (He et al., 1997) but not corrected for, as its amplitude was relatively small with rabbit psoas fibers. In the soleus fibers, however, this artifact was somewhat more clear but still its amplitude was smaller than 1% of the total amplitude of the fluorescence signal. In all experiments shown here the artifact was removed by subtracting an exponential from the data using the time constant given above, whose amplitude had been derived from the raw data.

The recordings shown in Figs. 1 and 2 were smoothed by calculating a running average (KaleidaGraph 3.0.1, Synergy Software, Reading, PA) using a window of 20 points (5 ms). Averaged values are given as means ± one standard error of the mean (S.E.M.) of n experiments. Differences were statistically tested by Student's t-test at a 0.05 level of significance ($P < 0.05$). Results from curve fitting are given ± standard error of the estimate (S.E.E.) using the S.E.M. values as relative weights.

RESULTS

P_i release and force in soleus fibers

Fig. 1 shows force and fluorescence recordings obtained in the presence of calcium (pCa 4.5) from two successive photolysis trials with 0.6 and 1.2 mM MDCC-PBP on the same soleus fiber at 15°C. Before the flash, the fiber was in

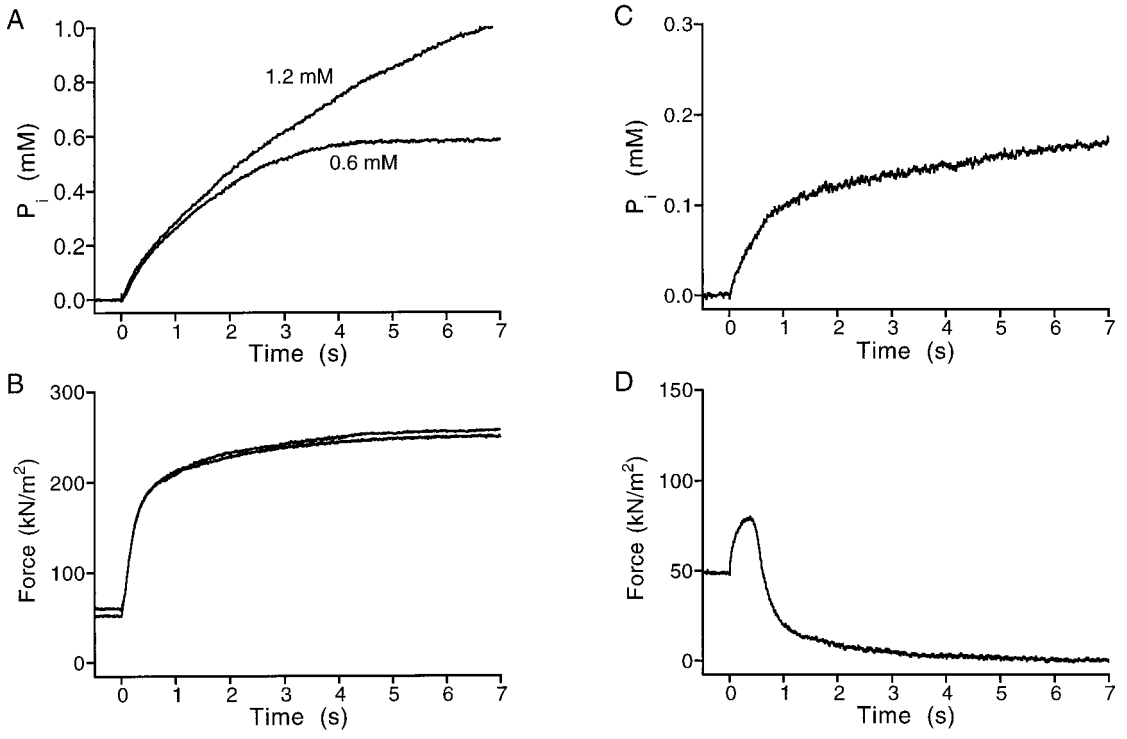

FIGURE 1 Force response and the amount of inorganic phosphate (P_i) released after photolysis of NPE-caged ATP in rabbit soleus muscle fibers. In *A* and *B*, recordings are shown from two successive photolysis trials in the presence of 0.6 and 1.2 mM MDCC-PBP in the presence of calcium (pCa 4.5) at 15°C. Initially the fiber was in the rigor solution containing Ca^{2+}. After photoliberation of 1.5 mM ATP, force increased rapidly toward the maximum isometric level. At the same time, the fluorescence signal from MDCC-PBP increased rapidly. P_i release in the muscle fiber was derived from the fluorescence intensity by the relationship given in Methods. P_i was released rapidly after photoliberation of 1.5 mM ATP until the probe saturated. ATP hydrolysis inside the fiber, however, continued; after a few seconds rigor force started to develop when all the ATP was used up (not shown). It can be seen that the early time course of P_i release was independent of the concentration of the probe used. In *C* and *D*, recordings are shown in the absence of calcium obtained with 0.6 mM MDCC-PBP. After photoliberation of 1.5 mM ATP, force transiently increased and thereafter the fiber relaxed and force returned to the passive baseline. Concomitantly, an increase in the fluorescence signal from the P_i-probe was observed. When force relaxation was complete, the fluorescence signal increased linearly with time for the 60 s of the measurements. Its slope reflects the basal rate of P_i release. All fluorescence traces were corrected for the *aci*-nitro signal (see Methods).

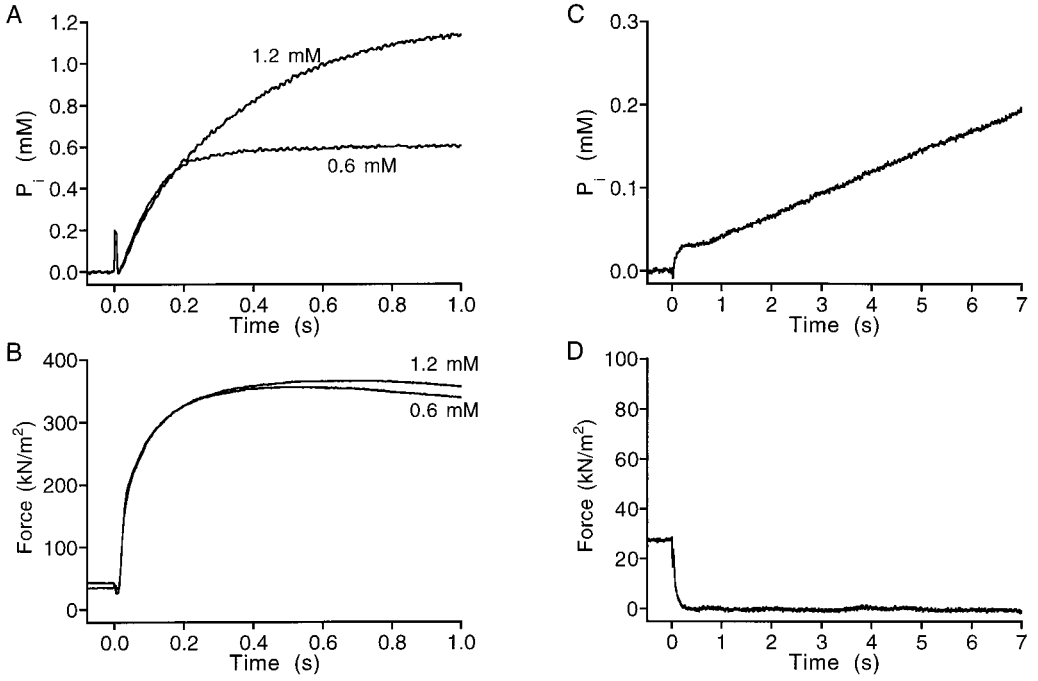

FIGURE 2 Force response and the amount of P_i released after photolysis of NPE-caged ATP in rabbit psoas muscle fibers at 15°C. In *A* and *B*, recordings are shown from two successive photolysis trials with 0.6 and with 1.2 mM MDCC-PBP in the presence of calcium (pCa 4.5) carried out in the same way as for soleus fibers (Fig. 1). Initially the fiber was in the rigor solution containing Ca^{2+}. After photoliberation of 1.5 mM ATP, force increased rapidly toward the maximum isometric level. At the same time, P_i was released rapidly until the probe saturated. It can be seen that the early time course of P_i release was independent of the concentration of the probe used. In *C* and *D*, a recording is shown in the absence of calcium obtained with the same fiber using 0.6 mM MDCC-PBP. Force transiently increased (not visible on this time scale); thereafter, the fiber relaxed. Concomitantly, an increase in the fluorescence signal from the P_i-probe was observed. When force relaxation was complete, the fluorescence signal increased linearly with time until the probe saturated. Its slope reflects the rate of P_i release.

the Ca^{2+}-containing rigor solution (pCa 4.5). Rigor force in soleus fibers ranged from 20 to 50 kN · m^{-2}. After photolytic release of ~1.5 mM ATP, force increased toward the maximum isometric level. At the same time, fluorescence increased rapidly until the probe saturated. ATP hydrolysis inside the fiber, however, continued; after a few seconds rigor force started to develop when all the ATP was used up (not shown). The results in Fig. 1 *A* indicate that the early time course of the fluorescence signal was independent of the concentration of the probe used. The maximum isometric force per cross-sectional area reached 250 kN · m^{-2}. In a set of experiments the maximum isometric force was 194 ± 23 kN · m^{-2} (n = 9) and the increase in force was well fit by a double exponential equation with rate constants of 7.1 ± 0.9 s^{-1} and 0.62 ± 0.11 s^{-1} (n = 16). The average rates found with the different probe concentrations were not significantly different. The amplitude of the fast component amounted to 60 ± 3% of the total increase in force. In Fig. 1, *C* and *D*, fluorescence and force signals for experiments in the absence of calcium are shown (pCa > 8). The fluorescence signal was obtained with 0.6 mM MDCC-PBP. A transient increase in force was observed, followed by a return of the force signal characteristic of the relaxed fiber (Goldman et al., 1984a). Concomitantly, an increase in the fluorescence signal was observed with an amplitude corresponding to 0.11 ± 0.02 mM P_i (n = 3). When force relaxation was complete, the fluorescence signal increased linearly with time until the probe saturated. The slope of this basal rate of P_i release corresponded to 11 ± 3 μM · s^{-1} in soleus fibers (n = 3).

The curvature of the fluorescence traces obtained in the presence of calcium (Fig. 1 *A*) shows that the rate of P_i release decreased gradually with time. P_i release as a function of time was well described by a single exponential over much of the time course, except for the initial fast phase and the approach to the final saturation of the probe. The average rate constant of the dominant exponential in the soleus trials (n = 15) was 0.48 ± 0.09 s^{-1}.

To describe the time course in more detail we determined the rate of P_i release at 0 (the initial rate) and at 0.15, 0.3, and 0.45 mM phosphate released. These values were chosen because they represent the amount of P_i released for the first, second, and third turnover of the actomyosin active sites assuming that the active site concentration is 0.15 mM (He et al., 1997) and because they could be determined both at 0.6 mM MDCC-PBP and at 1.2 mM MDCC-PBP.

The rate of P_i release in mM per second during successive turnovers is shown in Fig. 3. It started at an initial rate of 0.57 ± 0.05 mM · s^{-1} (n = 13) and declined to 0.20 ± 0.02 mM · s^{-1} at 0.45 mM P_i. In most fibers P_i release was studied both at 0.6 and at 1.2 mM MDCC-PBP. The values found with the different probe concentrations were not

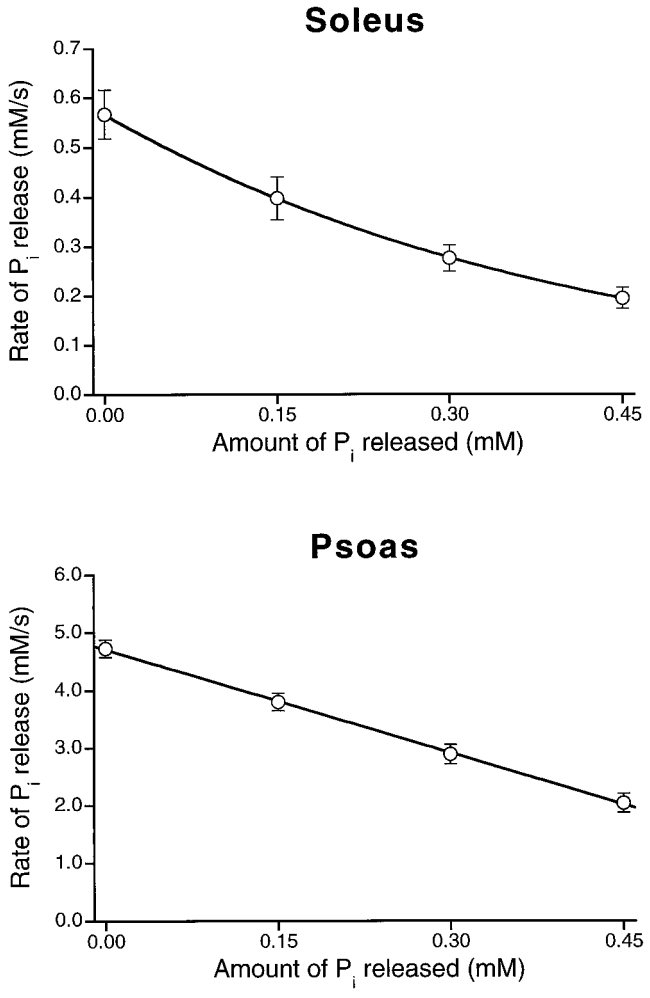

FIGURE 3 The initial rate of P_i release at subsequent turnovers of the whole cross-bridge population in soleus and psoas fibers. The initial rate of P_i release is plotted as a function of the amount of P_i released. The P_i concentration shown on the abscissa reflects the concentration of the MDCC-PBP with phosphate bound. The ordinate shows the average results (±S.E.M.) from the slopes derived from the calibrated fluorescence signals obtained with probe concentrations of 0.6 and 1.2 mM MDCC-PBP. The soleus results were fitted with an exponential relation of the form $Y = a \cdot \exp(-b \cdot [P_i])$ and the psoas results were fitted with a linear relation as described in the text.

significantly different. The line in the figure represents an exponential fit to the data points with decay constant (±S.E.E.) of 2.38 ± 0.29 mM^{-1}.

P_i release and force in psoas fibers

The experiments performed in soleus fibers were also carried out in psoas fibers using the same experimental conditions. Fig. 2, *A* and *B* show recordings obtained from two experimental trials in the presence of 0.6 and 1.2 mM MDCC-PBP on the same fiber in the presence of calcium at 15°C. After the photolytic release of ATP, force increased rapidly toward a maximum isometric level. The maximum isometric force per cross-sectional area amounted to 230 ± 11 $kN \cdot m^{-2}$ ($n = 13$), which was not significantly different from that in soleus fibers ($P = 0.15$). The increase in force (after the small initial dip) was fitted by means of a double exponential. The rate constants obtained, 89 ± 6 s^{-1} and 9.3 ± 0.6 s^{-1} ($n = 23$), were faster than in soleus fibers. The average rates found with the different probe concentrations were not significantly different. The amplitude of the fast component amounted to 51 ± 2% of the total increase in force. As expected, fluorescence increased more rapidly than in soleus fibers. The result in Fig. 2 *A* shows that also in psoas, the early time course of the fluorescence signal was independent of the concentration of the probe used (0.6 and 1.2 mM). In Fig. 2, *C* and *D*, the results are shown from a photolysis trial in the absence of calcium. The fiber relaxed and force returned to the resting value in a manner similar to that shown previously (Goldman et al., 1984a), without the prominent transient increase in force seen with soleus fibers. Concomitantly, an increase in the fluorescence signal from the P_i-probe was observed. After a small rapid phase with an amplitude corresponding to 0.03 mM P_i, fluorescence increased linearly with time until the probe saturated. The slope of this basal rate of P_i release corresponded to 23 ± 1 $\mu M \cdot s^{-1}$ ($n = 10$).

The rate of P_i release in the presence of Ca^{2+} decreased gradually with time. The mean rate constant of the dominant exponential in psoas was 5.2 ± 0.6 s^{-1} ($n = 23$). In addition, we determined the rate of P_i release at 0, 0.15, 0.3 and 0.45 mM phosphate released. The rate of P_i release in mM per second during the subsequent turnovers is shown in Fig. 3. It started at an initial rate of 4.7 ± 0.2 $mM \cdot s^{-1}$ ($n = 23$) and declined linearly by 0.88 ± 0.07 $mM \cdot s^{-1}$ per turnover. The values found with 0.6 and at 1.2 mM MDCC-PBP were not significantly different. Using an exponential fit to these data (as was done for soleus fibers) to describe the slowing of the rate of P_i release, gives a decay constant (±S.E.E.) of 1.76 ± 0.15 mM^{-1}, a value similar to that observed in soleus. A comparison between the results obtained on psoas fibers with those obtained on soleus fibers is given in Table 1.

TABLE 1 Overview of the results

Measured parameters	Soleus	Psoas	Units
Steady-state rate of P_i release in the absence of calcium	11 ± 3	23 ± 1	$\mu M \cdot s^{-1}$
Initial rate of P_i release in the presence of calcium	0.57 ± 0.05	4.7 ± 0.2	$mM \cdot s^{-1}$
Initial rate of P_i release in the presence of calcium for 150 μM active sites	3.8 ± 0.3	31.5 ± 1	s^{-1}
Rates of force development in the presence of calcium	7.1 ± 0.9 0.62 ± 0.11	89 ± 6 9.3 ± 0.6	s^{-1} s^{-1}
Deceleration of P_i release as a function of time	0.48 ± 0.09	5.2 ± 0.6	s^{-1}
Deceleration of P_i release as a function of P_i already released	2.38 ± 0.29	1.76 ± 0.15	mM^{-1}

Effects of ADP on P_i release and force in soleus fibers in the presence of Ca^{2+}

The effects of ADP on P_i release and force were investigated in five soleus fibers using an MDCC-PBP concentration of 1.2 mM at pCa 4.5 and 15°C. In each fiber the results in the presence of 0.5 mM ADP were compared with those in the presence of an ATP regenerating system, which causes conversion of the ADP formed back to ATP, and also with the control measurement without ATP regeneration. In Fig. 4 the results obtained on one fiber are shown. The rigor tension level before the photorelease of ATP is higher in the presence of 0.5 mM ADP. ADP also causes an increase in the maximum isometric force but a decrease in the rate of P_i release. Addition of the ATP regenerating system caused a reduction of the isometric force, but P_i release was not affected. Moreover, force started to decline when the P_i-probe saturated (data not shown), probably as a result of the subsequent rise in P_i concentration inside the fiber. The average results from this series of experiments showed relative to the control values an increase in maximum isometric force of 9 ± 4% when 0.5 mM ADP was added and a decrease in force of 10 ± 1% in the presence of an ATP regenerating system. In the presence of 0.5 mM added ADP, photolysis of ATP caused an initial rapid reduction in force, which was followed by a rapid rise in force as was observed recently by Horiuti et al. (1997). The minimum depended on the initial rigor force. It was reached ~20 ms after the flash and amounted to 40% of rigor force. The early time course is sensitive to ADP or to the initial rigor force, because the initial reduction in force is not visible in the presence of the ATP regenerating system and is small in the control experiment (no ATP regenerating system). In the presence of added ADP, the initial rate of P_i release and the rates of P_i release measured at 0.15, 0.30, 0.45, 0.60, and 0.75 mM P_i were reduced by 53–73% as compared to the values measured in the presence of an ATP regenerating system (Fig. 5). The ATP regenerating system caused a small increase in the averaged values of the rate of P_i release as compared to the control values. The averaged data points obtained in the presence of the ATP regenerating system did not differ significantly from the control data points. However, a paired *t*-test on the individual data points observed with and without the ATP-regenerating system showed a significant effect of the regenerating system compared to control.

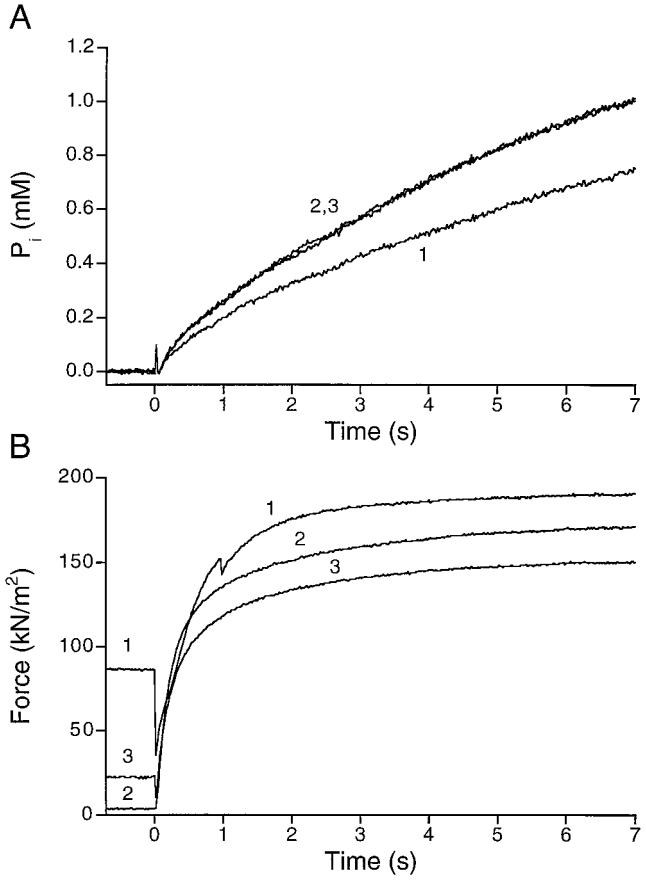

FIGURE 4 Effects of ADP on the force response and the amount of P_i released after photolysis of NPE-caged ATP in rabbit soleus muscle fibers. P_i release (*A*) and force (*B*) recordings from three successive photolysis trials: 1) in the presence and 2) absence of 0.5 mM added ADP, and 3) in the presence of an ATP regenerating system (PCr/CPK) performed at 15°C. In these experiments 1.2 mM MDCC-PBP and saturating calcium concentrations (pCa 4.5) were used. In *A*, the amount of P_i released is shown derived from the fluorescence signals obtained during these three trials. Note that the recording in the presence of an ATP regenerating system is almost identical to the recording under control conditions. The small discontinuity in the force recording (+0.5 mM ADP) in panel *B* probably originated from an abrupt change in the position of one of the T-clips used for mounting of the fiber in the experimental set-up.

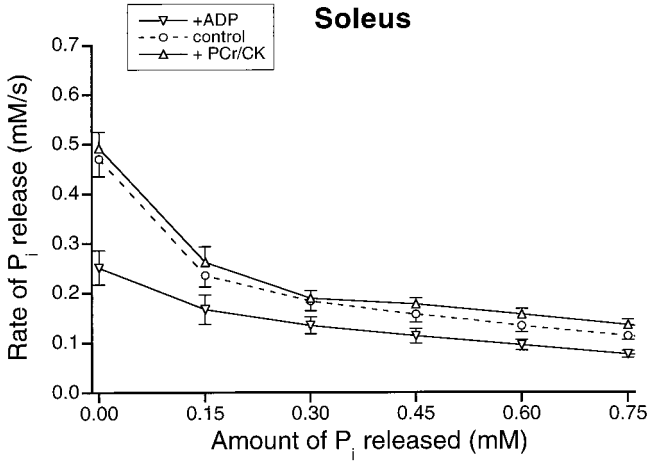

FIGURE 5 Effect of ADP on the rate of P_i release in soleus fibers at 15°C. In this figure the average results from paired experiments on five soleus fibers are shown. The format is the same as in Fig. 3, except that because 1.2 mM MDCC-PBP was used, more turnovers could be evaluated. The average values obtained in the presence of an ATP regenerating system (+PCr/CPK) did not differ significantly from the control values. The values obtained in the presence of 0.5 mM ADP were all significantly smaller ($P < 0.05$) than the control values.

Simulation of the effect of ADP on P_i release in soleus fibers

To get an insight in the effects of ADP on the rate of phosphate release, we calculated the ADP concentration inside the fibers at various times from P_i released, the kinetics of actomyosin interaction, and the properties of the ATP regenerating system. These calculations were based on averaged P_i release recordings during the ADP trials shown in Fig. 6 *A* and a simplified scheme for actomyosin interaction, in which M is myosin, AM is actomyosin, T is ATP, D is ADP, and P_i is inorganic phosphate.

$$AM + T \underset{r_1}{\overset{k_1}{\rightleftharpoons}} \boxed{MT \rightarrow AMDP_i} \xrightarrow{k_2} AMD + P_i \underset{r_3}{\overset{k_3}{\rightleftharpoons}} AM + D$$

Scheme 1

The creatine kinase-based re-synthesis of ATP was simulated by means of the rate equations described by Morrison and Cleland (1966) using the rate constants given by McFarland et al. (1994) and an equilibrium constant of creatine kinase at 15°C of 255 (Teage and Dobson, 1992). The model simulations were performed by means of the SIMCON program (National Simulation Resource, Center of Bioengineering, University of Washington, Seattle). It turned out that only the initial phase of P_i release could be described adequately with this model. Therefore, the curve fits shown were performed over the first 6 s after the laser flash. The values obtained were k_1, 8.6 $mM^{-1} \cdot s^{-1}$; r_1, 7.2 s^{-1}; k_2, 12.9 s^{-1}; k_3, 1.5 s^{-1}; and r_3, 3.0 $mM^{-1} \cdot s^{-1}$.

The simulated free ADP concentration inside the fiber is shown in Fig. 6. In the presence of the ATP regenerating system, the free ADP concentration remained low (<3 μM) for more than 10 s and the ATP concentration was well maintained. However, the observed rate of P_i release continuously declined (Fig. 6 *A*), but the simulated rate of P_i release remained steady. This shows that the decline in P_i release cannot be wholly attributed to accumulation of ADP. Under control conditions, the ADP concentration increased gradually to 1.2 mM at the end of the simulation (16 s) and ATP concentration declined accordingly. Addition of 0.5 mM ADP caused an approximately 0.5 mM offset on this latter ADP curve.

In the absence of the ATP regenerating system, and even more markedly upon addition of 0.5 mM ADP, the observed decrease in the rate of P_i release was more pronounced than when the ADP concentration was kept in the micromolar range by the ATP regenerating system (Fig. 6 *A*). This indicates that the rate of P_i release does depend on ADP accumulation. However, for ADP to account for all the observed slowing down of the rate of P_i release in the presence of the ATP regenerating system, one would need to consider that the presence of ADP in micromolar concentrations had a significant effect on the P_i release rate, even in the presence of millimolar concentration of ATP.

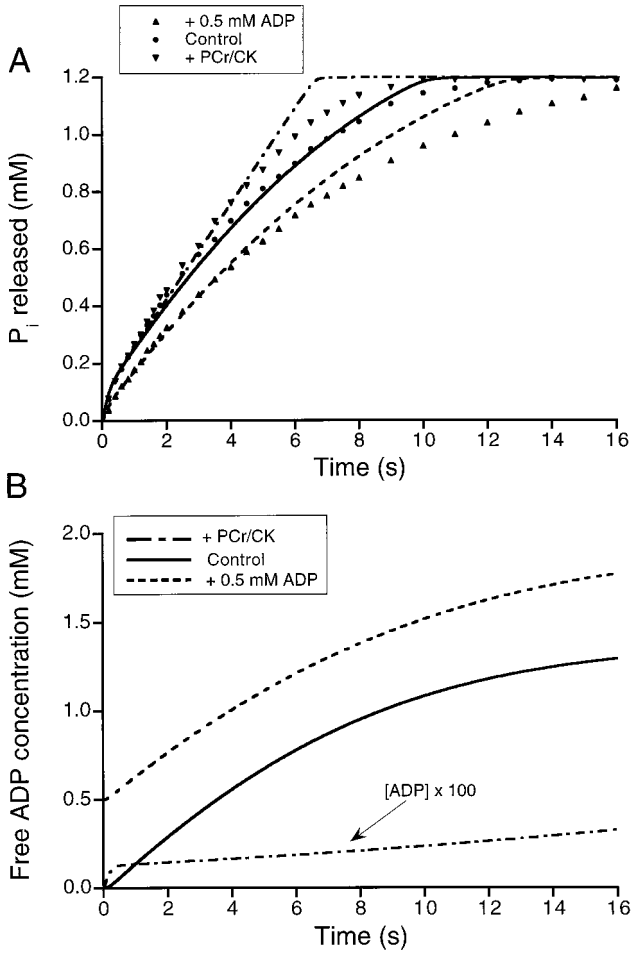

FIGURE 6 Model simulations of the amount of P_i released after photolysis of 1.5 mM NPE-caged ATP. In *A*, averaged data points obtained from paired experiments on five soleus fibers are shown under control conditions, in the presence of 0.5 mM added ADP, and in the presence of an ATP regenerating system (PCr/CPK). The lines denote the results from a computer simulation based on the kinetic scheme of cross-bridge interaction (Scheme 1), fitted to the data points during the first 6 s after photolysis of 1.5 mM caged ATP. In the simulations the effects of saturation of the P_i-probe and ADP re-synthesis were taken into account. Curve fits were performed by nonlinear least-mean-square optimization to the three sets of averaged data points shown, simultaneously. The rate for ATP association (7.2 s^{-1}) was chosen such that the ATP dissociation constant was identical to the value of 1.2 mM^{-1} obtained by Wang and Kawai (1996). Lower values (i.e., larger dissociation constants) provided an almost indistinguishable but slightly better fit. In *B*, the free ADP concentration is shown calculated from the simulations shown in *A*.

Influence of end-compliance

Upon photolysis of caged ATP in the presence of calcium, the fiber starts to develop force. This will cause sarcomere shortening because of the compliance present in the connections between the fiber and the set-up. We tried to minimize this end-compliance by cross-linking the ends of the fiber with glutaraldehyde. However, to obtain an estimate of the amount of sarcomere shortening, a control experiment on a soleus fiber was performed in which sarcomere length was monitored by means of laser diffraction.

The results from this experiment are shown in Fig. 7. It can be seen in this figure that internal shortening occurs corresponding to ~60 nm per half sarcomere, i.e., ~5% of the initial sarcomere length (2.4 μm). Approximately half of the internal shortening occurs during the first second after the laser fired and the maximum velocity of shortening (30 nm · half sarcomere^{-1} · s^{-1}) was reached during this initial rapid phase of force development.

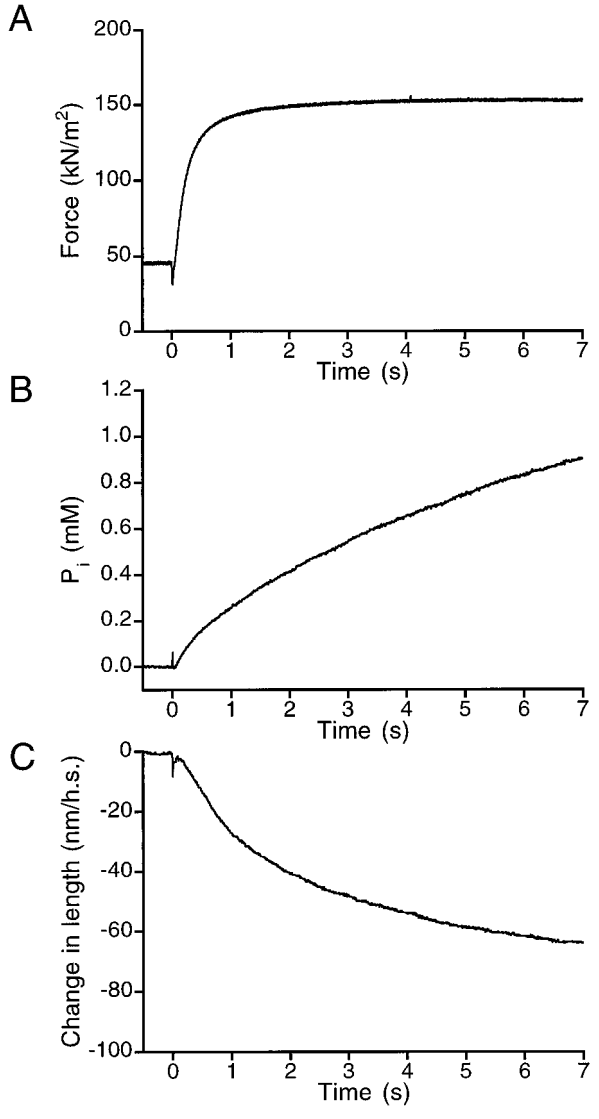

FIGURE 7 Sarcomere length changes during a photolysis trial in the presence of calcium. Force (*A*), P_i release (*B*), and sarcomere length change in nm per half sarcomere (nm/h.s.) (*C*) recordings from a photolysis trial on a soleus fiber without added ADP or an ATP regenerating system at 15°C. In this experiment 1.2 mM MDCC-PBP and a saturating calcium concentration (pCa 4.5) were used. Force development during the first second after the flash was accompanied by a rapid phase of sarcomere shortening at a velocity of 30 nm · half sarcomere^{-1} · s^{-1}. The change in sarcomere length observed just before the MDCC-PBP saturated occurred at a velocity of only 0.5 nm · half sarcomere^{-1} · s^{-1} (not shown).

DISCUSSION

The results of this study indicate that the initial rate of phosphate release in isometrically contracting soleus fibers is higher than the steady-state rate of ATP hydrolysis determined previously (Potma et al., 1994b; 1995; see below). The comparison between slow and fast fibers suggests that the deceleration of phosphate release is an intrinsic property of the contractile apparatus.

Maximum isometric force development

The maximum isometric force per cross-sectional area under control conditions was 194 ± 23 kN · m^{-2} in soleus and 230 ± 11 kN · m^{-2} in psoas. These values are higher than the values found in previous comparative studies of the rate of ATP consumption (Stienen et al., 1992; Potma et al., 1994b, 1995) at 15°C and in other studies. For instance, Ferenczi (1986) found in psoas fibers that isometric force at 13.4°C was 140 kN · m^{-2}. The high isometric force found here is largely attributable to the very low phosphate concentration (<1 μM) inside the fibers during the measurements. This resulted from the use of the MEG/PNPase system to minimize P_i contamination of the solutions as well as of the fiber, and because the P_i-probe had a high affinity for P_i (K_d = 0.15 μM) and hence effectively prevented P_i accumulation inside the fiber until the probe was saturated. It has been shown (e.g., Chase and Kushmerick, 1988; Cooke and Pate, 1985; Iwamoto, 1995; Kawai et al., 1987; Millar and Homsher, 1990, 1992; Nosek et al., 1990; Stienen et al., 1992) that phosphate depresses force at millimolar concentrations and above, but the effect of removal of P_i was only investigated in the work of He et al. (1997), and more recently by Pate et al. (1998). The observed decline in force after the P_i-probe saturated in the presence of the ATP regenerating system is also most likely a consequence of P_i accumulation in the fiber once the P_i binding sites on MDCC-PBP have become saturated. Other, but minor, factors that may contribute to the high isometric force are the buildup of ADP up to 1.5 mM (cf. Cooke and Pate, 1985; Chase and Kushmerick, 1995) and the decline in ATP concentration (e.g., Glyn and Sleep, 1985) and also small differences in ionic strength of the solutions.

P_i release and force relaxation in the absence of calcium

In the absence of calcium, a rapid phase of P_i release was observed during force relaxation from rigor. This early phase was followed by a slower linear phase of P_i release, reflecting basal ATPase activity of 11 ± 3 μM · s^{-1} in soleus and of 23 ± 1 μM · s^{-1} in psoas fibers. These values are comparable to the basal ATPase activity derived from NADH absorbance measurements, using a coupled enzyme system, of 5 ± 2 μM · s^{-1} in soleus and 23 ± 4 μM · s^{-1} in psoas fibers (Potma et al., 1994b). Initial force relaxation occurred rapidly and was followed by a transient increase in

force, a hump, typical for caged ATP photolysis experiments in the presence of small amounts of ADP (cf. Goldman et al., 1984a; Thirlwell et al., 1994). The hump in soleus fibers was more pronounced and occurred later than in psoas fibers. This latter observation is in agreement with the results of Horiuti et al. (1997), who also provided additional evidence suggesting that (in the rat) slow fibers are more sensitive to ADP than fast fibers. Such tighter binding is consistent with the notion that the greater economy of slow fibers is brought about by the slow release of ADP from actomyosin, which results in a low ATPase rate at the expense of shortening velocity while maintaining force (cf. Fuglsang et al., 1993).

The rate of P_i release in soleus fibers during the transient tension rise and the slow relaxation immediately following it was found to be higher than when the fiber was fully relaxed (Fig. 1 *C*), providing further evidence that the transition from rigor to relaxed muscle involves at least partial activation of the contractile machinery. Indeed, the rate of P_i release at the maximum force reached (0.5 s after the flash) was ~40% of the rate observed at the same time in the presence of Ca^{2+}, whereas maximum force ($-Ca^{2+}$) was 50% of the force observed in the presence of calcium at that time. The hump has been attributed to cooperative binding of cross-bridges (Goldman et al., 1984a). According to our measurements these cycling cross-bridges split ATP at a similar rate, as observed in the presence of a saturating calcium concentration.

P_i release and force development at saturating calcium concentration

At 15°C, the initial rate of P_i release was 0.57 ± 0.05 mM · s^{-1} in soleus and 4.7 ± 0.2 mM · s^{-1} in psoas. Assuming a myosin head density in the skinned fibers of 0.15 mM (Ferenczi et al., 1984; He et al., 1997) this corresponds to a rate of P_i release expressed per myosin of 3.8 s^{-1} in soleus and 31.5 s^{-1} in psoas. The values in psoas fibers fit between the values found using the P_i-probe by He et al. (1997) at 12 and 20°C. These values are considerably higher than the steady-state values found for ATP consumption both in soleus and in psoas. Potma et al. (1994b, 1995) obtained values for the steady-state rate of ATP consumption at 15°C of 0.05 and 0.4 mM · s^{-1} in soleus and psoas, respectively. These latter values agree well with previous steady-state estimates based on heat production and oxygen consumption during isometric contractions in tetanically stimulated intact muscles (Gibbs and Gibson, 1972; Crow and Kushmerick, 1982).

Force development was well described by a double exponential equation with rate constants of 7.1 ± 0.9 s^{-1} and 0.62 ± 0.11 s^{-1} in soleus fibers and of 89 ± 6 s^{-1} and 9.3 ± 0.6 s^{-1} in psoas fibers. It is of interest to note that in both fiber types, the slower of the two rates is similar to the rate constant of the exponential dominating P_i release (0.48 and 5.2 s^{-1} for soleus and psoas fibers, respectively). This may indicate that the slow phase is related to a redistribution of cross-bridges between attached states with different force whereas the fast phase might reflect the initial attachment and force generation of cross-bridges.

Earlier data of Ferenczi et al. (1984) concerning the time course of MgATP cleavage after photolysis of NPE-caged ATP were interpreted in terms of a rapid burst of P_i formation followed by a steady-state ATPase of 1.9 s^{-1} in rabbit psoas fibers at 12°C. He et al. (1997) indicated that the previous data were consistent with a smaller burst of protein-bound ADP and a subsequent nonlinear rate of ADP formation. However, the estimated rate of P_i release during the first second after photolysis of NPE caged ATP was still half the value observed in He et al. (1997) and in the psoas fibers in this study. The notion that the P_i burst, if present at all, is quite small in comparison with the myosin head concentration is consistent with the data presented in this study in psoas as well as in soleus fibers.

Effects of ADP on P_i release and force development

In the absence of an ATP regenerating system, continuous ATP hydrolysis results in the stoichiometrically coupled breakdown of ATP and formation of ADP. It has been shown previously that a reduction in ATP concentration has little effect on ATPase activity or force production (e.g., Glyn and Sleep, 1985). However, ADP in the millimolar range potentiates isometric force and depresses isometric ATPase activity with a K_i of ~0.2 mM (Sleep and Glyn, 1986). It has been reported also that ADP alters cross-bridge kinetics (Wang and Kawai, 1996; Horiuti et al., 1997), who found K_m values of 40–60 μM in rabbit and rat soleus fibers and that ADP depresses rigor force in rabbit psoas fibers with a K_m of 18 μM (Dantzig et al., 1991). The effects of ADP on P_i release and force development in psoas fibers were investigated by He et al. (1997). They found that 0.5 mM ADP caused a small reduction in the initial rate of P_i release (23 ± 7%). In addition, they observed that the initial rate of P_i release in the presence of an ATP regenerating system was identical to that under control conditions (at 12°C), although the ATP regenerating system was not capable of eliminating ADP accumulation during the period of high ATPase activity. Our results in soleus fibers are very similar to the findings of He et al. (1997). With 0.5 mM ADP, we find a reduction in the rate of P_i release over the complete time course investigated of ~35%. The comparison between P_i release under control conditions with that in the presence of an ATP regenerating system revealed that P_i release in the control fibers might be slightly depressed during the late phases of the photolysis trial when more than 0.3 mM ADP had accumulated (Fig. 6, *A* and *B*). Taken together, these observations indicate that a considerable amount of ADP (>0.3 mM) is required to slow P_i release. In the presence of an ATP regenerating system, ADP is maintained at or below 3 μM (Fig. 6 *B*). This implies that

the initial slowing of P_i release, which is fitted by the model simulations, represents a transient phase because of the distribution of cross-bridges over the different states. AMD cross-bridges will be formed at the expense of AM (rigor) cross-bridges present before photolysis of NPE-caged ATP (Scheme 1). The rate constants involved in this redistribution obtained from the model simulation (ATP dissociation and P_i release) are similar to literature values (cf. Potma et al., 1994b; 1995), but the ADP association constant (i.e., $r_3/k_3 = 2\ mM^{-1}$) is less than the value of 18 mM^{-1} obtained by Wang and Kawai (1996) at 20°C. In addition, it should be noted that the subsequent slowing of relaxation could not be fitted by the model simulations. As explained below, we attribute this ADP-sensitive slowing to a decline in the rate of cross-bridge detachment with time or the number of cross-bridge turnovers. It should be noted, however, that ADP accumulation per se cannot explain the difference between the rates of P_i release observed in this study and the steady-state ATPase measurements, because the ADP concentration in these latter experiments amounts to 10–50 μM (Potma and Stienen, 1996).

Effects of internal shortening

Compliance located in connections of the fibers to the experimental set-up will introduce internal shortening of sarcomeres during force development, which may cause an increase in the rate of ATP hydrolysis, and hence in the rate of P_i release due to the Fenn effect (cf. Woledge et al., 1985). We minimized the amount of internal shortening by cross-linking the ends of the fiber segments with glutaraldehyde. Experiments in psoas fibers at 7°C in which sarcomere length changes were recorded and P_i release was studied at different speeds of isovelocity shortening (He and Ferenczi, in preparation) indicated that during the early phase of force development internal shortening may occur by ~5% of the fiber length at a speed 10% or less of the maximum shortening velocity. According to these experiments, internal shortening could account for only 10% of the initial slowing of the rate of P_i release. The control experiment on a soleus fiber shown in this study (Fig. 7) was in agreement with these estimates because it also revealed an internal sarcomere shortening of ~5% and a maximum speed of shortening (30 nm · half sarcomere^{-1} · s^{-1}), which was <10% of the velocity of unloaded shortening (~600 nm · half sarcomere^{-1} · s^{-1} in soleus fibers at 15°C). This is not expected to lead to a significant increase in the ATPase activity above the value observed during an isometric contraction (e.g., Fig.5.5*A* in Woledge et al., 1985; Reggiani et al., 1997).

Another source of internal shortening resides in the compliance of the actin and myosin filaments. Recent x-ray studies (Huxley et al., 1994; Wakabayashi et al., 1994) indicate that this would account for an internal shortening with maximum force development of ~0.2%. The previous estimates based on an end compliance causing a change in sarcomere length of ~5%, indicate that the influence of filament compliance on the speed of phosphate release is small.

Estimation of the transition rates in the cross-bridge cycle

In previous studies (Potma et al., 1994b, 1995) a three-state model was used to simulate the pH and P_i dependence of force development and the steady-state rate of ATP utilization in skinned rabbit soleus and psoas muscle fibers (Scheme 2). To explore the consequences of the high P_i release rates found in this study we used the rates and equations derived by Potma et al. as a starting point. We shall demonstrate below that the high P_i release rate and the subsequent decline found are compatible with most of the rate constants used, but that they necessitate a change in one of the rate constants associated with cross-bridge detachment.

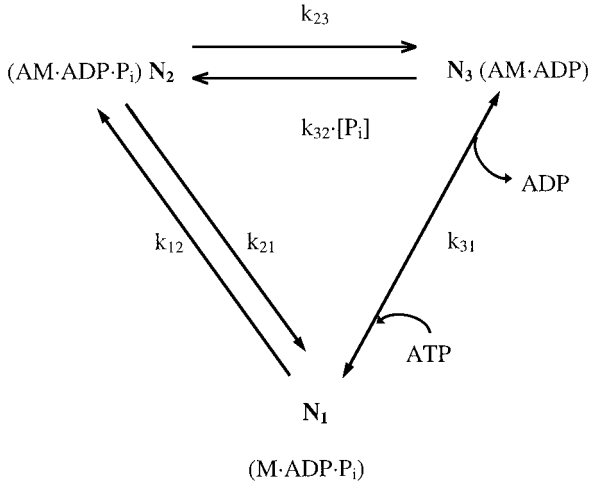

Scheme 2

where M = myosin, AM = actomyosin, N_1 = detached cross-bridges, N_2 = no- or low-force-producing cross-bridges, N_3 = force-producing cross-bridges, k_{12} = attachment rate, k_{21} = reverse attachment rate, k_{23} = rate of myosin isomerization and/or P_i release, $k_{32} \cdot [P_i]$ = reverse rate of myosin isomerization and/or P_i release, and k_{31} = rate of ADP release and/or cross-bridge detachment.

Because in the present study the free P_i concentration is very low, the backward rate constant $k_{32} \cdot [P_i]$ is considered negligibly small. In the isometric steady state, the ATPase activity per myosin head is given by (cf. Potma et al., 1994b)

$$\begin{aligned} \text{ATPase} &= k_{31} \cdot N_3 \\ &= k_{12}k_{23}k_{31}/(k_{12}k_{23} + k_{12}k_{31} + k_{21}k_{31} + k_{23}k_{31}). \end{aligned} \quad (2)$$

The values used previously were, for soleus, $k_{12} = 3\ s^{-1}$; $k_{21} = 6.9\ s^{-1}$; $k_{23} = 3\ s^{-1}$ and $k_{31} = 0.32\ s^{-1}$; and for psoas, $k_{12} = 75\ s^{-1}$; $k_{21} = 64\ s^{-1}$; $k_{23} = 20\ s^{-1}$; and $k_{31} = 2.8\ s^{-1}$. These rate constants result in a steady-state ATPase rate of 0.25 s^{-1} and 2.0 s^{-1} per myosin head for soleus and

psoas fibers, respectively, which are much smaller than the initial rates of P_i release found in this study. In Scheme 1, the maximum velocity of P_i release is obtained when all cross-bridges are present in the AM · ADP · P_i state (N_2). Let this situation occur immediately (or with a short lag) after photolysis of NPE-caged ATP, e.g., because of synchronized action of almost instantaneous detachment from rigor ($N_3 \rightarrow N_1$) and reattachment ($N_1 \rightarrow N_2$) of cross-bridges. To account for the initial rate of P_i release k_{23} is set to 3.8 s^{-1} in soleus and 31.5 s^{-1} in psoas fibers, i.e., the initial rates of P_i release expressed per myosin head found in this study. These values are similar to the values of 3 and 20 s^{-1} found by Potma et al. (1994b, 1995). However, to maintain the high velocity of P_i release for some time after the flash, k_{31} should be larger than the steady-state values found by Potma et al. This can be seen from the steady-state solution in Scheme 2 where the ATPase rate equals the initial high rate of P_i release. Substitution of the values for the initial rate of P_i release, and the k_{12} and k_{21} values used previously in Eq. 2, yields an equation with two unknowns k_{31} and k_{23}, and therefore a family of solutions for k_{31} and k_{23}.

For soleus fibers, the first observation from the simulations was that using the value for k_{12} of 3 s^{-1}, the maximum rate of P_i release could not be maintained in the steady state. In the present simulations, a slightly higher value of 7–10 s^{-1} provides a better fit to the data. To arrive at a steady-state ATPase rate of 3.8 s^{-1}, k_{31} as well as k_{23} should be at least 20 s^{-1}. Hence, the slowing of the overall cross-bridge cycling from the initial rate of P_i release toward the steady-state ATPase rate implies a major slowing of k_{31} by at least a factor of 60 and possibly also some slowing (by a factor of 5) of k_{23}.

In psoas fibers the value of k_{12} of 64 s^{-1} is compatible with an initial rate of P_i release of 31.5 s^{-1}. The steady-state solution of Scheme 2 for a cross-bridge turnover rate of 31.5 s^{-1}, however, requires a high value for k_{31} of 100-1000 s^{-1} in psoas and a value for k_{23} of at least 20 s^{-1}. Therefore, the approximately fivefold slowing of the overall cross-bridge cycling from the initial rate of P_i release toward the steady-state ATPase rate implies a major slowing of k_{31} by at least a factor of 40, and possibly also some slowing (by a factor of 6) of k_{23}.

Interpretation of the results

The initial rate of P_i release after photolysis of NPE-caged ATP is ~10-fold faster than the steady-state ATPase rate obtained previously both in fast and in slow skeletal muscle fibers. The rate of P_i release decelerates with time in both fiber types. The deceleration can be expressed as a function of the amount of P_i split or as a function of the number of cross-bridge turnovers. Saturation of the P_i binding protein did not allow us to study the approach toward the steady-state level. The rates involved in cross-bridge cycling necessary to explain the marked slowing of the overall turnover are compatible with the values found in the literature (Wang and Kawai, 1996; Goldman et al. 1984a, b; Zhao and Kawai, 1993; Potma et al., 1994b, 1995) except for the apparent rate of cross-bridge detachment (presumably an isomerization preceding ADP release, e.g., Geeves et al., 1984). This marked slowing of the rate-limiting step in the cross-bridge cycle has not been observed in studies of the contractile proteins in solution nor in previous kinetic studies in isometrically contracting skinned muscle fibers or in myofibrils (Lionne et al., 1996). The decay in the rate of ATP hydrolysis with time, or of turnover number, may highlight a mechanism to reduce energy consumption of the muscle fiber in the isometric state, whereas during the development of force, ATP hydrolysis is not down-regulated, perhaps to achieve the maximum rate of force rise.

Recently, Josephson and Edman (1998) showed that, in frog muscle fibers at 1–3°C, maximum velocity of shortening early during a tetanus was as much as 30% greater than at the tetanic plateau. They indicated that this observation was in agreement with the Huxley (1957) model and that it could be attributed to the initial recruitment of cross-bridges during the first 30 ms after the onset of activation. This process might play a role during the initial phase of the P_i transient, although in our experiments cross-bridges depart from the rigor state.

It should be emphasized that the rates of P_i release and ATP hydrolysis presented in this paper are expressed per myosin head assuming that all heads participate. If, as proposed recently (e.g., Howard, 1997), structural constraints for cross-bridge attachment would limit the number of cross-bridges involved, the values for the rates derived would increase accordingly. This would not affect the relative comparison made between the rates of P_i release and of the steady-state ATPase because both would be scaled equally. The presence of these structural constraints needs to be rigorously tested. However, if present, they open the possibility for the following tentative explanation for the observed decline in the rate of P_i release. It is possible that in rigor muscle the fraction of attached heads is larger than during an isometrically contracting muscle (cf. Linari et al., 1998), especially if rigor bridges are less rigid than active bridges (Howard, 1997) and hence they might occupy actin binding sites which are structurally less favorable because of the helical pitch of the actin filament. Thus, active force development upon photolytic release of ATP could be associated with a reduction in the number of active cross-bridges that could contribute to the slowing of P_i release, without a change in the chemical probability of P_i release.

We thank Dr. D. R. Trentham for valuable discussions and Dr. M. R. Webb and Dr. M. Brune for the phosphate binding protein and the purification of phosphocreatine kinase.

This work was supported by the European Union (Human Capital and Mobility, Grant ERBCHRXCT 940606).

REFERENCES

Bershitsky, S., A. Tsaturyan, O. Bershitsky, G. Mashanov, P. Brown, M. Webb, and M. A. Ferenczi. 1996. Mechanical and structural properties underlying contraction of skeletal muscle fibers after partial 1-ethyl-3-[3-(dimethylamino)propyl]carbodiimide cross-linking. *Biophys. J.* 71: 1462–1474.

Brune, M., J. L. Hunter, J. E. T. Corrie, and M. R. Webb. 1994. The direct, real-time measurement of rapid inorganic phosphate release using a novel fluorescent probe and its application to actomyosin subfragment 1 ATPase. *Biochemistry*. 33:8262–8271.

Chase, P. B., and M. J. Kushmerick. 1988. Effects of pH on contraction of rabbit fast and slow skeletal muscle fibers. *Biophys. J.* 53:935–946.

Chase, P. B., and M. J. Kushmerick. 1995. Effects of physiological ADP concentration on contraction of single fibers from rabbit fast and slow muscles. *Am. J. Physiol.* 268:C480–C489.

Cooke, R., and E. Pate. 1985. The effects of ADP and phosphate on the contraction of muscle fibers. *Biophys. J.* 48:789–798.

Corrie, J. E. T. 1994. Thiol-reactive fluorescent probes for protein labelling. *J. Chem. Soc., Perkin Trans.* 1:2975–2982.

Corrie, J. E. T., Y. Katayama, G. P. Reid, M. Anson, and D. R. Trentham. 1992. The development and application of photosensitive caged compounds to aid time-resolved structure determination of macromolecules. *Phil. Trans. R. Soc. Lond. A*. 340:233–244.

Corrie, J. E. T., and G. P. Reid. 1995. Site-specific labelling of caged-ATP with deuterium or ^{18}oxygen. *J. Labelled Compd. Radiopharm.* 36: 289–300.

Crow, M. T., and M. J. Kushmerick. 1982. Chemical energetics of slow- and fast-twitch muscles of the mouse. *J. Gen. Physiol.* 79:147–166.

Dantzig, J. A., M. G. Hibberd, D. R. Trentham, and Y. E. Goldman. 1991. Cross-bridge kinetics in the presence of MgADP investigated by photolysis of caged ATP in rabbit psoas muscle fibres. *J. Physiol.* 432: 639–680.

Ferenczi, M. A. 1986. Phosphate burst in permeable muscle fibers of the rabbit. *Biophys. J.* 50:471–477.

Ferenczi, M. A., Z.-H. He, R. K. Chillingworth, M. Brune, J. E. T. Corrie, D. R. Trentham, and M. R. Webb. 1995. A new method for the time-resolved measurement of phosphate release in permeabilized muscle fibers. *Biophys. J.* 68:191s--193s.

Ferenczi, M. A., E. Homsher, and D. R. Trentham. 1984. The kinetics of magnesium-adenosine triphosphate cleavage in skinned muscle fibres of the rabbit. *J. Physiol.* 352:575–599.

Fuglsang, A., A. Khromov, K. Török, A. V. Somlyo, and A. P. Somlyo. 1993. Flash photolysis studies of relaxation and cross-bridge detachment: higher sensitivity of tonic than phasic smooth muscle to MgADP. *J. Muscle Res. Cell Motil.* 14:666–673.

Geeves, M. A., R. S. Goody, and H. Gutfreund. 1984. Kinetics of acto-S1 interaction as a guide to a model for the crossbridge cycle. *J. Muscle Res. Cell Motil.* 5:351–361.

Gibbs, C. L., and W. R. Gibson. 1972. Energy production of rat soleus muscle. *Am. J. Physiol.* 223:864–871.

Glyn, H., and J. Sleep. 1985. Dependence of adenosine triphosphatase activity of rabbit psoas muscle fibres and myofibrils on substrate concentration. *J. Physiol.* 365:259–276.

Goldman, Y. E., M. G. Hibberd, and D. R. Trentham. 1984a. Relaxation of rabbit psoas muscle fibres from rigor by photochemical generation of adenosine-5′-triphosphate. *J. Physiol.* 354:577–604.

Goldman, Y. E., M. G. Hibberd, and D. R. Trentham. 1984b. Initiation of active contraction by photogeneration of adenosine-5′-triphosphate within rabbit psoas muscle fibres. *J. Physiol.* 354:605–624.

Goldman, Y. E., and R. M. Simmons. 1984. Control of sarcomere length in skinned muscle fibres of Rana temporaria during mechanical transients. *J. Physiol.* 350:497–518.

He, Z.-H., R. K. Chillingworth, M. Brune, J. E. T. Corrie, D. R. Trentham, M. R. Webb, and M. A. Ferenczi. 1997. ATPase kinetics on activation of permeabilized isometric fibres from rabbit and frog muscle: a real time phosphate assay. *J. Physiol.* 501.1:125–148.

Horiuti, K., N. Yagi, and S. Takemori. 1997. Mechanical study of rat soleus muscle using caged ATP and X-ray diffraction: high ADP affinity of slow cross-bridges. *J. Physiol.* 502.2:433–447.

Howard, J. 1997. Molecular motors: structural adaptations to cellular functions. *Nature*. 389:561–567.

Huxley, A. F. 1957. Muscle structure and theories of contraction. *Progr. Biophys. Biophys. Chem.* 7:255–318.

Huxley, H. E., A. Stewart, H. Sosa, and T. Irving. 1994. X-ray diffraction measurements of the extensibility of actin and myosin filaments in contracting muscle. *Biophys. J.* 67:2411–2421.

Iwamoto, H. 1995. Strain sensitivity and turnover rate of low force cross-bridges in contracting skeletal muscle fibers in the presence of phosphate. *Biophys. J.* 68:243–250.

Josephson, R. K., and K. A. P. Edman. 1998. Changes in the maximum speed of shortening of frog muscle fibres in a tetanic contraction and during relaxation. *J. Physiol.* 507.2:511–525.

Kawai, M., K. Güth, K. Winnikes, C. Haist, and J. C. Rüegg. 1987. The effect of inorganic phosphate on the ATP hydrolysis rate and the tension transients in chemically skinned rabbit psoas fibers. *Pflügers Arch.* 408:1–9.

Linari, M., I. Dobbie, M. Reconditi, N. Koubassova, M. Irving, G. Piazzesi, and V. Lombardi. 1998. The stiffness of skeletal muscle in isometric contraction and rigor: the fraction of myosin heads bound to actin. *Biophys. J.* 74:2459–2473.

Lionne, C., M. Brune, M. R. Webb, F. Travers, and T. Barman. 1995. Time resolved measurements show that phosphate release is the rate limiting step on myofibrillar ATPases. *FEBS Lett.* 364:59–62.

Lionne, C., F. Travers, and T. Barman. 1996. Mechanochemical coupling in muscle: attempts to measure simultaneously shortening and ATPase rates in myofibrils. *Biophys. J.* 70:887–895.

McFarland, E. W., M. J. Kushmerick, and T. S. Moerland. 1994. Activity of creatine kinase in a contracting mammalian muscle of uniform fiber type. *Biophys. J.* 67:1912–1924.

Millar N. C., and E. Homsher. 1990. The effect of phosphate and calcium on force generation in glycerinated rabbit skeletal muscle fibers. *J. Biol. Chem.* 265:20234–20240.

Millar, N. C., and E. Homsher. 1992. Kinetics of force generation and phosphate release in skinned rabbit soleus muscle fibers. *Am. J. Physiol.* 262:C1239–C1245.

Morrison, J. F., and W. W. Cleland. 1966. Isotope exchange studies of the mechanism of the reaction catalyzed by adenosine triphosphate: creatine phosphotransferase. *J. Biol. Chem.* 241:673–683.

Nosek, T. M., J. H. Leal-Cardoso, M. McLaughlin, and R. E. Godt. 1990. Inhibitory influence of phosphate and arsenate on contraction of skinned skeletal and cardiac muscle. *Am. J. Physiol.* 259:C933–C939.

Pate, E., K. Franks-Skiba, and R. Cooke. 1998. Depletion of phosphate in active muscle fibers probes actomyosin states within the powerstroke. *Biophys. J.* 74:369–380.

Potma, E. J., and G. J. M. Stienen. 1996. Increase in ATP consumption during shortening in skinned fibres from rabbit psoas muscle: effects of inorganic phosphate. *J. Physiol.* 496.1:1–12.

Potma, E. J., G. J. M. Stienen, J. P. F. Barends, and G. Elzinga. 1994a. Myofibrillar ATPase activity and mechanical performance of skinned fibres from rabbit psoas muscle. *J. Physiol.* 474.2:303–317.

Potma, E. J., I. A. van Graas, and G. J. M. Stienen. 1994b. Effects of pH on myofibrillar ATPase activity in fast and slow skeletal muscle fibers of the rabbit. *Biophys. J.* 67:2404–2410.

Potma, E. J., I. A. van Graas, and G. J. M. Stienen. 1995. Influence of inorganic phosphate and pH on ATP utilization in fast and slow skeletal muscle fibers. *Biophys. J.* 69:2580–2589.

Reggiani, C., E. J. Potma, R. Bottinelli, M. Canepari, M. A. Pellegrino, and G. J. M. Stienen. 1997. Chemo-mechanical energy transduction in relation to myosin isoform composition in skeletal muscle fibres of the rat. *J. Physiol.* 502.2:449–460.

Sleep, J., and H. Glyn. 1986. Inhibition of myofibrillar and actomyosin subfragment 1 adenosinetriphosphatase by adenosine 5′-diphosphate, pyrophosphate, and adenyl-5′-yl imidodiphosphate. *Biochemistry*. 25: 1149–1154.

Stienen, G. J. M., M. C. M. Roosemalen, M. G. A. Wilson, and G. Elzinga. 1990. Depression of force by phosphate in skinned skeletal muscle fibers of the frog. *Am. J. Physiol.* 259:C349–C357.

Stienen, G. J. M., P. G. A. Versteeg, Z. Papp, and G. Elzinga. 1992. The mechanical properties of skinned rabbit psoas and soleus muscle fibres

during lengthening: the effects of phosphate and Ca^{2+}. *J. Physiol.* 451:503–523.

Teage, W. E., and G. P. Dobson. 1992. Effect of temperature on the creatine kinase equilibrium. *J. Biol. Chem.* 267:14084–14093.

Thirlwell, H., J. E. T. Corrie, G. P. Reid, D. R. Trentham, and M. A. Ferenczi. 1994. Kinetics of relaxation from rigor of permeabilized fast-twitch fibers from the rabbit using a novel caged ATP and apyrase. *Biophys. J.* 67:2436–2447.

Wakabayashi, K., Y. Sugimoto, H. Tanaka, Y. Ueno, Y. Takezawa, and Y. Amemiya. 1994. X-ray diffraction evidence for the extensibility of actin and myosin filaments during muscle contraction. *Biophys. J.* 67: 2422–2435.

Walker, J. W., G. P. Reid, and D. R. Trentham. 1989. Synthesis and properties of caged nucleotides. *Methods Enzymol.* 172:288–301.

Wang, G., and M. Kawai. 1996. Effects of MgATP and MgADP on the cross-bridge kinetics of rabbit soleus slow-twitch muscle fibers. *Biophys. J.* 71:1450–1461.

Webb, M. R., M. G. Hibberd, Y. E. Goldman, and D. R. Trentham. 1986. Oxygen exchange between P_i in the medium and water during ATP hydrolysis mediated by skinned fibers from rabbit skeletal muscle. *J. Biol. Chem.* 261:15557–15564.

Woledge, R. C., N. A. Curtin, and E. Homsher. 1985. Energetic aspects of muscle contraction. *Monographs of the Physiological Society.* 41: 167–275.

Zhao, Y., and M. Kawai. 1993. The effect of the lattice spacing change on cross-bridge kinetics in chemically skinned rabbit psoas muscle fibers. *Biophys. J.* 64:197–210.